

Fragmentation of Relativistic Gold by Various Target Nuclei

C. J. Waddington, J. R. Cummings¹, and B. S. Nilsen²,

University of Minnesota, Minneapolis, MN 55455, USA

¹*Washington University, St. Louis,*

²*Van de Graff Lab., Ohio State University*

Abstract

We have recently studied the interactions of gold nuclei, $^{197}_{79}\text{Au}$, at eight different energies between 0.9 and 4.0 A GeV, in targets ranging in mass from hydrogen to lead. This paper combines the results of these studies with earlier measurements at higher and lower energies. We discuss the production of fragments with charges, Z , between 81 and 50. The systematic trends found have allowed us to improve previously developed empirical relations which predict the cross sections in any target or energy for the production of fragments with $77 \geq Z \geq 67$. Fragments with single and double charge pickup are observed in all targets at all energies. Fragments which have lost a single charge represent a special case. The energy variations of the total cross sections and the approach with increasing energy to limiting fragmentation are studied. Details of the experimental techniques and data analysis will be described elsewhere.

1. Measurements:

Total charge changing cross sections, σ_{H} , were measured at each energy and in each target. The energy dependence of σ_{H} is shown in Figure 1 for all targets, together with linear fits between 0.9 and 4.0 A GeV of the form:

$$\sigma_{\text{H}} = \sigma_0 + \alpha \cdot E_{\text{beam}} \quad \text{Eq. 1}$$

It can be seen from these new results that σ_{H} is essentially constant for the lighter targets, but that for the heavier targets there is a small but significant decrease in σ_{H} as E increases to 4.0 A GeV. This decrease in σ_{H} does not continue out to 10.6 A GeV. Instead, there are increases, which are greatest for the heaviest targets, presumably due to the effects of electromagnetic dissociation.

The cross sections, σ_{H} , for charge changes, Z , at the different energies in a hydrogen target are shown in Figure 2. Also shown on this figure are the low energy data from Cummings *et al.* (1990), and the high energy data from Geer *et al.* (1995). This plot has the new results shown as solid symbols and the previous data as open symbols. This plot, while very busy, illustrates the general power law nature of the relation between σ_{H} and $|Z|$ at higher energies and the deviations from a power law for such a light target at the lower energies. Heavier targets follow power laws much more closely. The energy dependence of the hydrogen cross sections can be seen in Figure 1, which shows the hydrogen cross sections as a function of energy for each Z between -1 and -10 . This figure shows that in general for small Z , σ_{H} decreases with increasing E , but that for large Z , σ_{H} reaches a maximum at an intermediate energy.

2. Analysis:

The partial cross sections in hydrogen for $E \geq 5.0$ A GeV in all the targets and for $|Z| \geq 12$, can be fitted by one or two power law relations in energy, depending on the target and Z .

$$\sigma(Z, E, A_T) = \sigma_0(Z, A_T) E^{n(Z, A_T)} \text{ mb} \quad \text{Eq. 2}$$

where $\sigma_0(Z, A_T)$ is the value of the cross section at 1.0 A GeV, and $n(Z, A_T)$ is the exponent of the energy variation. These parameters may also depend on a critical energy, E_c , representing a transition

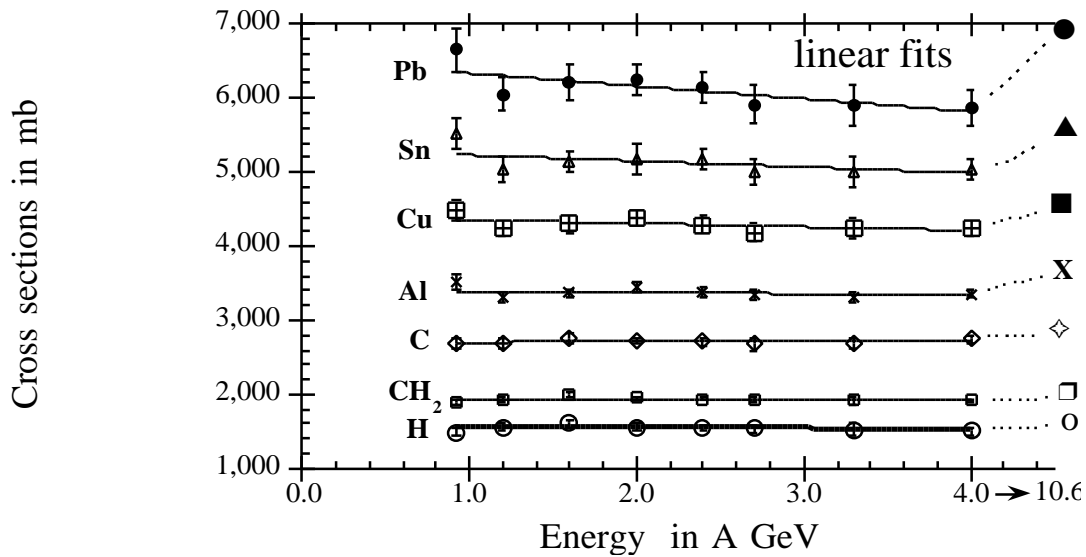


Fig.1 The total charge changing cross sections for each target as a function of energy. Note the break in the energy scale between 4 and 10.6 A GeV.

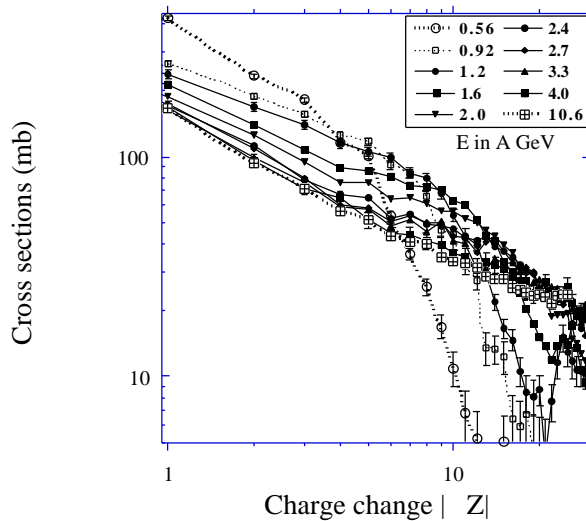


Fig. 2 Partial cross sections, σ , in mb, for gold on a hydrogen target, as a function of charge change, $|Z|$, at all available energies.

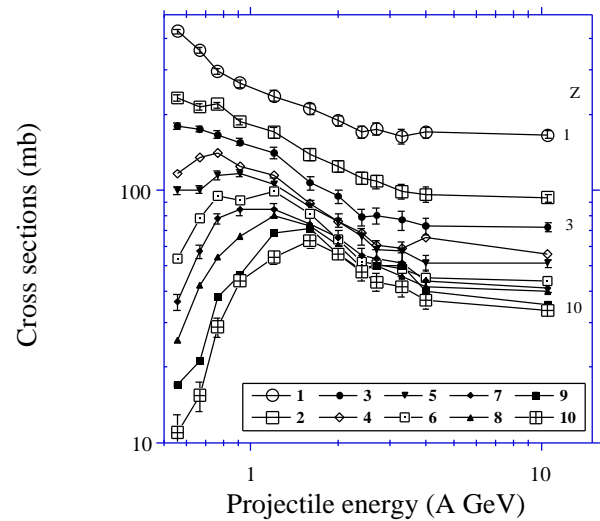


Fig. 3 Partial cross sections, σ , in mb, for gold on a hydrogen target, as a function of beam energy for different fragments with $|Z|$ between 1 and 10.

from a positive to a negative exponent. For hydrogen and $|Z| > 3$ it appears that E_c increases slowly from 1.0 to 1.3 A GeV as $|Z|$ increases. For $E_c \approx E \approx 5.0$ A GeV or for $|Z| \leq 3$, both σ_0 and n can be represented as power laws in $|Z|$ of the form:

$$\sigma_0 = (267 \pm 3) |Z|^{(-0.553 \pm 0.012)} \text{ mb} \quad \text{Eq. 3}$$

$$n = (-0.452 \pm 0.019) |Z|^{(0.143 \pm 0.033)} \quad \text{Eq. 4}$$

At $E < E_c$ and for $|Z| \geq 4$, σ_0 and n can both be represented by relations of the form:

$$\sigma_0 = (359 \pm 14) \exp(|Z| (-0.217 \pm 0.005)) \text{ mb} \quad \text{Eq. 5}$$

$$n = (4.79 \pm 0.29) \log(|Z| (0.26 \pm 0.009)) \quad \text{Eq. 6}$$

It can be seen that the change in behavior at the critical energy is quite drastic. The exponent of the energy dependence varies from being positive at low energies to negative at higher energies. In all the fits to the data and to the power law parameters there are acceptable values of χ^2 for each of the individual fits. A comparison between all the measured cross sections in hydrogen and those predicted from Eqs. 2 - 6 is shown in Figure 4.

A comparison of the results from these predictions and those obtained from the revised version derived in earlier work, Nilsen et al (1995), shows that this new formalism is significantly better at matching the available measured values for gold nuclei. Using the present predictions, 91% of the values agree to within 20% of the measured values for $2 \leq |Z| \leq 12$. The previous formalism only matched 76% of a data set, more limited in energy but with more projectiles, to within 20%.

For the targets heavier than hydrogen, it is not necessary to invoke a critical energy. All the cross sections for $|Z| \geq 12$ and $E \geq 5.0$ A GeV for each target can be fitted by one power law, although with individual values of $\sigma_0(A_T)$ and $n(Z, A_T)$.

A global fit to the data is given by:

$$\sigma(Z, E, A_T) = \sigma_0(A_T) |Z|^{A_T} E^{(a+bA_T)} |Z|^{(c+dA_T)} \text{ mb} \quad \text{Eq. 7}$$

The fitted values of these various constants with their uncertainties are given in the Table.

Application of this global fit to all the available data for $2 \leq |Z| \leq 12$ and $0.5 \leq E \leq 10.6$ A GeV shows that the fit is a good representation of the data. 60% of all the predicted values are within 5% of the measured values, 88% are within 10%. Alternatively, 65% of the predictions are within one standard deviation of the measured values and 93% are within 2 standard deviations. Given the uncertainties in the constants in the Table, the predictions appear to be excellent. Note that these predictions are significantly better than those derived above for the hydrogen target.

If we neglect those terms with small constants then:

$$\sigma(Z, E, A_T) = (196 A_T^{0.1}) Z^{-0.8} E^{(0.25)} Z^{-0.15} \text{ mb} \quad \text{Eq. 8}$$

From this form we note that σ_0 is only weakly dependent on A_T , but does show a clear dependence on E for $E \geq 4.0$ A GeV when $|Z| \geq 12$. Thus:

$$\sigma(Z, E, A_T) = A_T^{0.1}; \quad Z^{-0.8}; \quad E^{-0.25} Z^{-0.15} \quad \text{for } E \geq 4.0 \text{ A GeV and } 2 \leq |Z| \leq 12.$$

The E dependence is not a function of A_T , showing that it is not appropriate to consider the total energy in the center of mass as an organizing variable in these peripheral interactions.

In each run it was possible to identify a clear peak of ^{80}Hg nuclei, resulting from pickup of a single charge, "plus 1's", Nilsen et al (1994). The cross sections for these are shown in Fig. 3. In most runs it was also possible to distinguish a small number of ^{81}Tl nuclei, double charge pickup, "plus 2's". The cross sections for the production of these nuclei are less than 1.0 mb. It has only been possible to detect a significant number of these rare nuclei due to the larger numbers of interactions that were obtained during these latest runs at the AGS.

The above relations can be used to predict the cross sections needed in calculations of the effects introduced during propagation of UH cosmic ray nuclei through the interstellar space. In addition, allowances can be made for the effects of local matter such as overlying detectors or an atmosphere.

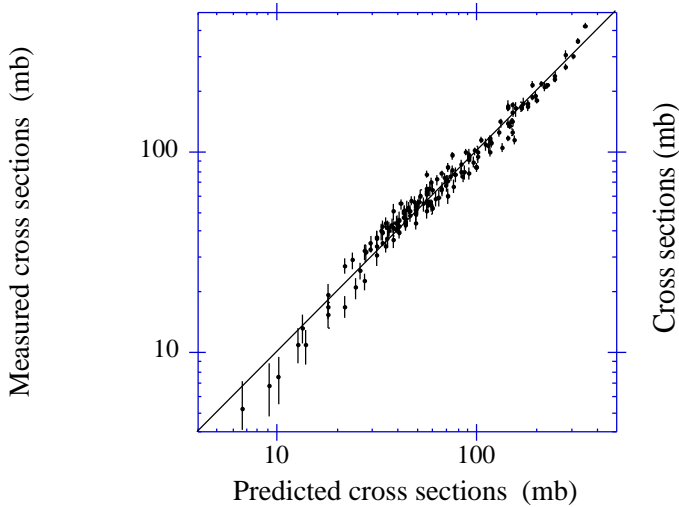


Fig. 4 Comparison between measured partial cross sections of gold in hydrogen for Z between -1 and -12 and the values predicted from Eqs. 2 to 6.

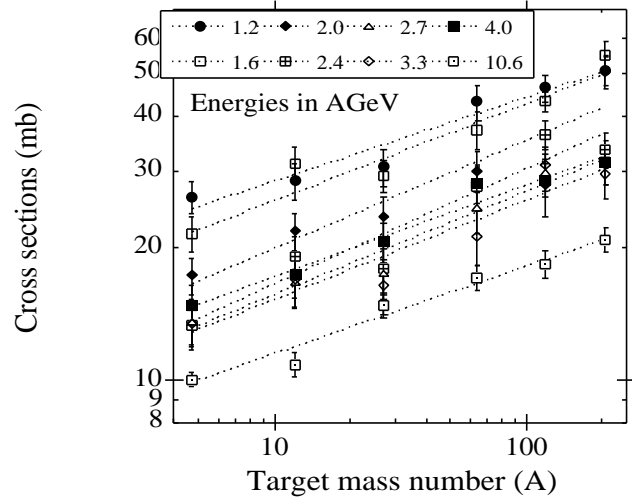


Fig. 5 Cross sections, in mb, for the production of $_{80}\text{Hg}$ nuclei from $_{79}\text{Au}$ nuclei at various energies, as a function of target mass number, A

Table: Values of constants in Eq. 7

| Constant | Value | \pm | Constant | Value | \pm |
|----------|--------|-------|----------|---------------------|------------------|
| | 196 | 5 | a | -0.253 | 0.014 |
| | 0.108 | 0.008 | b | $-(0.6 \cdot 10^0)$ | $(5 \cdot 10^0)$ |
| | -0.788 | 0.017 | c | -0.143 | 0.034 |
| | -0.017 | 0.007 | d | $(4 \cdot 10^0)$ | $(5 \cdot 10^0)$ |

Refs:

B. S. Nilsen, C. J. Waddington, W. R. Binns, J. R. Cummings, T. L. Garrard, L. Y. Geer and J. Klarmann, 1994, Phys. Rev., C50, 1065
 B. S. Nilsen, C. J. Waddington, J. R. Cummings, T. L. Garrard, and J. Klarmann, 1995, Phys. Rev., C52, 3277
 L. Y. Geer, J. Klarmann, B. S. Nilsen, C. J. Waddington, W. R. Binns, J. R. Cummings and T. L. Garrard, 1995, Phys. Rev., C52, 334
 C. J. Waddington, J. R. Cummings, T. L. Garrard and B. S. Nilsen, 1999, July, Ap. J.

Acknowledgements: This work supported by NASA under Grants NASA/NAG5-5077 and NAS5-5113. We are indebted to J. Klarmann, and Paul Hink for assistance during these runs, and to the staff of the AGS for generous exposures and help beyond the line of duty during the Blizzard of '96